Ground-state phase diagram of the quantum $J_1 - J_2$ model on the honeycomb lattice

Fabio Mezzacapo[1] and Massimo Boninsegni[2]

[1] *Max-Planck-Institut für Quantenoptik, Hans-Kopfermann-Str.1, D-85748, Garching, Germany*
[2] *Department of Physics, University of Alberta, Edmonton, Alberta, Canada T6G 2E1*

(Dated: February 9, 2012)

We study the ground-state phase diagram of the quantum $J_1 - J_2$ model on the honeycomb lattice by means of an entangled-plaquette variational ansatz. Values of energy and relevant order parameters are computed in the range $0 \leq J_2/J_1 \leq 1$. The system displays classical order for $J_2/J_1 \lesssim 0.2$ (Néel), and for $J_2/J_1 \gtrsim 0.4$ (collinear). In the intermediate region, the ground-state is disordered. Our results show that the reduction of the half-filled Hubbard model to the model studied here does not yield accurate predictions.

Frustrated quantum antiferromagnets are a subject of current intense research, whose study is rendered even more timely by recent, intriguing proposals of possible experimental realizations with ultracold atoms.[1] Frustration can arise either from the geometry of the system, or from competing interactions, and can lead to the stabilization of novel, exotic (magnetic and non-magnetic) phases of matter.

A prototypical spin model, featuring interaction-induced frustration, is the spin-1/2 antiferromagnetic (AF) Heisenberg Hamiltonian in presence of next-nearest-neighbor (NNN) coupling (usually referred to as the J_1-J_2 model):

$$J_1 \sum_{\langle i,j \rangle} \mathbf{S}_i \cdot \mathbf{S}_j + J_2 \sum_{\langle\langle i,j \rangle\rangle} \mathbf{S}_i \cdot \mathbf{S}_j \qquad (1)$$

where $\mathbf{S}_i$ is a spin-1/2 operator associated to the ith lattice site and the first (second) summation runs over NN (NNN) sites. Periodic boundary conditions (PBC) are assumed.[2]

Model (1) has been extensively studied on the square lattice,[3] and has more recently elicited great interest on the honeycomb one,[4–12]. For $J_2 = 0$ (i.e., with no NNN interaction), the ground state (GS) of (1) features AF long-range (Néel) order on both these two bipartite lattices.[13] When $J_2 > 0$ the system is frustrated. Néel order remains, for sufficiently small values of J_2, but as J_2 grows different phases, including disordered ones, become energetically competitive. For example, on the square lattice the GS displays magnetic long-range order (albeit of different types) for small and large value of J_2, while the nature of the GS in the intermediate region (i.e., $J_2 \sim 0.5$) is still under debate.[3] On the honeycomb lattice, due to its lower coordination number with respect to the square one, the disruptive effect of quantum fluctuations on magnetic order is enhanced, as confirmed by the value of the sublattice magnetization, which in the unfrustrated case is approximatively 10% smaller on the honeycomb than on the square lattice[13].

Studies of the magnetic phase diagram of the J_1-J_2 model on the honeycomb lattice, based on different computational approaches, have yielded conflicting physical scenarios. For example, it is unclear if the GS of
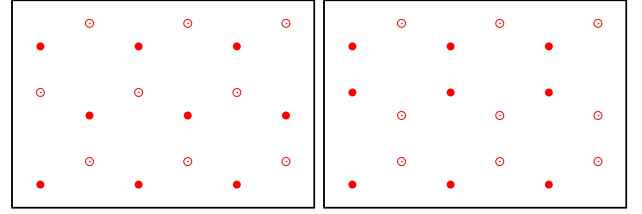

FIG. 1: (color on line). Schematic representation of the honeycomb lattice, with the two different definitions of sublattices (A and B) corresponding to Néel (left) and collinear (right) orders.

the system is disordered ("spin liquid") for any value of J_2, and even the nature of ordered phases remains controversial.[4–10] Exact diagonalization (ED) of (1) on small lattices (up to 42 sites), yields evidence of AF Néel order for $J_2 \lesssim 0.2$. For $0.2 \lesssim J_2 \lesssim 0.4$ the system is predicted to be in a plaquette valence-bond crystalline phase, while, for larger values of J_2, a collinear phase (not easy to characterize on small lattices) has been suggested[6] (see Fig. 1). The physical picture emerging from ED, whose predictive power is clearly affected by finite-size limitations, must be assessed by calculations performed on systems of much larger size, in order to carry out a reliable extrapolation of the relevant physical properties to the thermodynamic limit. Series expansions yield, for instance, a similar physical scenario, the main difference being a GS with spiral magnetic order found in the intermediate region.[10]

Quantum Monte Carlo (QMC) approaches yield numerically exact estimates for very large system sizes at $J_2 = 0$, but are not applicable in presence of frustration due to the well-known "sign" problem. Conversely, variational Monte Carlo (VMC) methods are by definition free of such problem, and suffer from no significant size limitation. Of course, they are also approximate, their accuracy depending on the choice of the variational wave function (WF). A recent variational investigation of the J_1-J_2 Hamiltonian on the honeycomb lattice, predicts the disappearance of Néel order at $J_2 \simeq 0.08$, a dimerized rotational symmetry-breaking phase for $J_2 \gtrsim 0.3$ and a

spin-liquid GS in the intermediate region.[4] It should be noted that, while in studies based on ED the presence of order of different kinds is assessed by a computation of relevant order parameters, the conclusions of Ref. 4 are mainly based on the comparison of energy estimates yielded by variational WF's corresponding to differently ordered, or disordered GS's.

Given the qualitative disagreement between ED and the only existing variational study, two basic aspects that still need be clarified are *a*) the type of magnetic order (if any) of phase(s) that occur as Néel order is suppressed on increasing J_2, and *b*) the nature of the GS for $J_2 \gtrsim 0.4$. Also of interest is the value of J_2 at which the Néel order vanishes, which according to Ref. 4 is in quantitative agreement with that found for the half-filled Hubbard model.[14]

In this paper, we report results of a variational study of the GS phase diagram of (1) on the honeycomb lattice, using the variational family of entangled-plaquette states (EPS).[15] This is a general ansatz, which has been shown to yield accurate estimates of GS observables for quantum spin lattice Hamiltonians, including frustrated ones.[15,16] The goal of this work is to determine the phase diagram of the model of our interest by direct estimation of the values of various order parameters, extrapolated to the thermodynamic limit. Specifically, besides GS energies we also compute sublattice magnetizations and dimer-dimer correlation functions. We find AF Néel order up to $J_2 \lesssim 0.2$, whereas for $J_2 \gtrsim 0.4$ the AF order is collinear; for $0.2 \lesssim J_2 \lesssim 0.4$ the GS is instead disordered.

An exhaustive description of the EPS class of states can be found in Refs. 15 and 16. We merely wish to stress that the EPS WF has been applied to a variety of lattice spin Hamiltonians, always providing results of accuracy at least comparable to (or better than) that afforded by different numerical techniques or variational WF's.

In this study, given the specific magnetic orders (see Fig. 1) that we aim at identifying, the appropriate phase factors have been incorporated in the general ansatz. Our numerical calculations have been carried out for lattices of size as large as $N = 324$ sites. For each lattice size and value of J_2, we independently and systematically optimize the EPS WF, by progressively increasing the size of our plaquettes (i.e., the number l of lattice sites that a plaquette comprises). Both the WF optimization and the evaluation of various physical quantities are achieved via the variational Monte Carlo method. We extrapolate to the thermodynamic limit the estimates obtained on finite lattices of different sizes, for a given plaquette size, and then, asses the dependence of our results on the plaquette size.

Table I shows the GS energy per site $e \equiv E/N$ for a lattice comprising $N = 100$ sites, for different values of J_2; estimates are shown corresponding to different plaquette sizes. Also shown for comparison are the variational estimates reported in Ref. 4 by Clark *et al.* For all values of J_2, our energy estimates are lower than those of Ref.

TABLE I: GS energy per site as a function of J_2 for a system of size $N = 100$ with PBC. Data for different plaquette-size l are shown. Variational estimates from Ref. 4 are also reported for comparison. Statistical errors (in parentheses) are on the last digit.

J_2	$l = 9$	$l = 16$	$l = 18$	Ref. 4
0.0	-0.54155(7)	-0.54418(6)		-0.537901(9)
0.1	-0.49049(5)	-0.49349(6)		-0.488209(3)
0.15	-0.46744(5)	-0.47087(4)		-0.469448(2)
0.2	-0.44599(4)	-0.45004(6)	-0.45145(4)	-0.450687(4)
0.3	-0.40936(6)	-0.41580(7)	-0.41751(4)	-0.41688(1)
0.4	-0.40650(5)	-0.41185(5)		-0.41125(1)
0.5	-0.42432(5)	-0.42940(6)		-0.42808(2)
0.6	-0.45248(5)	-0.45712(4)		
0.7	-0.48519(4)	-0.48989(5)		-0.47377(3)
0.8	-0.52112(6)	-0.52610(5)		
0.9	-0.55928(4)	-0.56489(5)		
1.0	-0.59917(5)	-0.60534(5)		

4. For $J_2 \leq 0.1$, as well as for large J_2, we obtain lower variational estimates than those of Ref. 4 already with plaquettes of size l=9. Plaquettes of larger size, typically $l = 16$ (and up to $l = 18$ for values of $0.2 \lesssim J_2 \lesssim 0.3$), are needed in order to improve on the variational energy estimates of Ref. 4 in the remaining cases. This illustrates the main quality of the EPS ansatz, namely that it can be systematically improved by increasing the size of the plaquette, yielding energy estimates of accuracy, typically higher than that afforded by other trial WF's.

Estimates of the GS energy per site for various values of J_2 and different plaquette size l are shown in Fig. 2 (left part), as a function of the system size. Extrapolation to the thermodynamic limit of numerical estimates obtained with the same l has been performed by assuming the functional scaling form $e(N, l, J_2) = e(\infty, l, J_2) + \alpha(l, J_2)N^{-3/2}$. Extrapolated values, therefore, depend on the size l of the plaquette utilized. Since by construction expectation values (of *any* observable) must approach the *exact* GS values in the limit of large plaquette size, the question is how to obtain a reliable estimate for such a limit, based on those obtained with relatively small plaquettes. While in principle calculations with ever increasing plaquette size should be carried out, in order to observe numerical convergence of results, currently available computer resources limit the largest plaquette size for which this procedure can be implemented in practice. As it turns out, however, results for both the energy and for the relevant magnetic order parameters obtained with plaquettes of size up to l=16, lend themselves to simple numerical extrapolations.[17]

An example of this procedure is illustrated in the right part of Fig. 2, showing energy estimates extrapolated to the thermodynamic limit i.e., $e(\infty, l, J_2)$, as a function of the plaquette size. We assume that $e(\infty, l, J_2)$ can be expanded in powers of $l^{-1/2}$ and fit the data using the smallest number of powers. As shown in the figure, the values of $e(\infty, l, J_2)$ fall on a straight line when
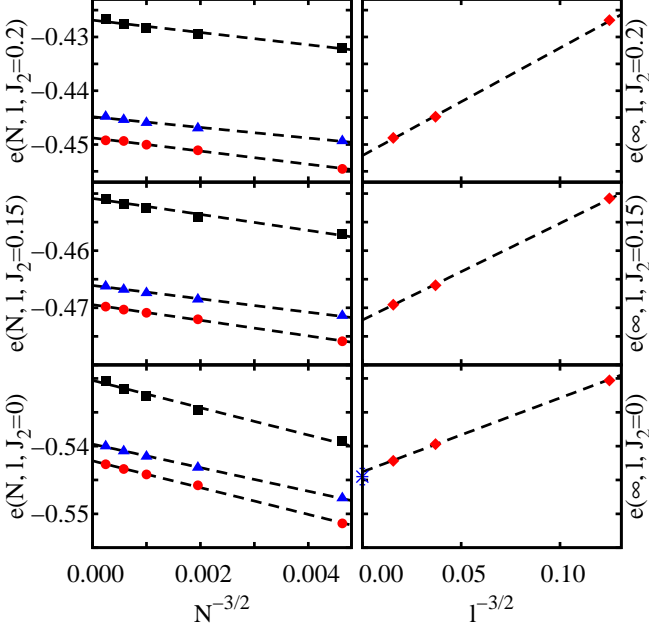
FIG. 2: (color on line). Left: GS energy per site of the $J_1 - J_2$ model on the honeycomb lattice with PBC, as a function of the system size. Estimates are obtained with N plaquettes of $l = 4$ (boxes), $l = 9$ (triangles) and $l = 16$ (circles) sites. Each dashed line is a fit to numerical data with the same l value. Right: GS energy per site, extrapolated to the thermodynamic limit, as a function of the plaquette-size. Each dashed line is a fitting function linear in $l^{-3/2}$ (see text). The QMC estimate in the $J_2 = 0$ case is also shown for comparison (star).[18]
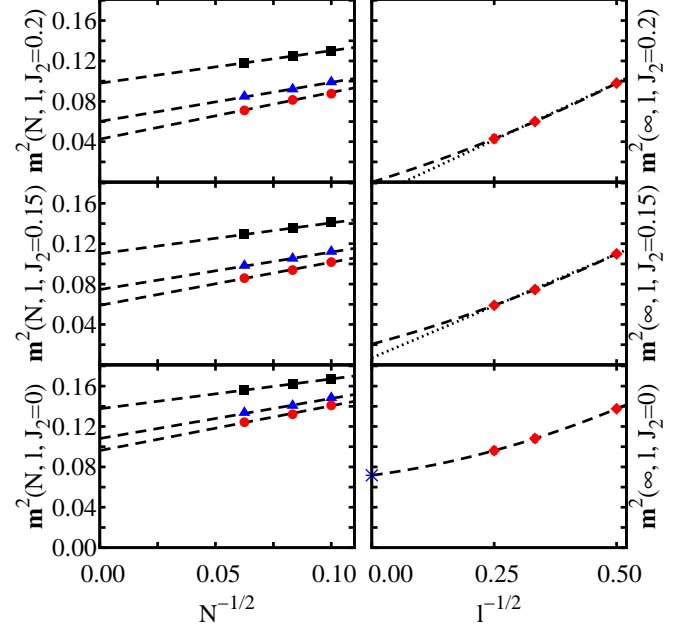
FIG. 3: (color on line). Left: Néel SSM of the $J_1 - J_2$ model on the honeycomb lattice with PBC, as a function of the system size. Estimates are obtained with N plaquettes of $l = 4$ (boxes), $l = 9$ (triangles) and $l = 16$ (circles) sites. Each dashed line is a fit to numerical data with the same l value (see text). Right: Néel SSM, extrapolated to the thermodynamic limit, as a function of the plaquette-size. Lines are functions bult to infer the l dependence of our data (see text). The QMC estimate in the $J_2 = 0$ case is also shown for comparison (star).[13]

plotted versus $l^{-3/2}$, i.e., an excellent fit to the data is obtained with a single power (dashed lines); in any case, the extrapolated value does not change appreciably on including additional terms. For $J_2 = 0$, this procedure leads to an estimate in agreement with that obtained by QMC[13,18] (essentially exact in this case).

The cogent observable, in order to assess the presence of magnetic order in the J_1-J_2 Hamiltonian, is the squared sublattice magnetization (SSM), defined as

$$\mathbf{m}^2(N) = \left\langle \frac{1}{N^2}(\sum_{i\in A} \mathbf{S}_i - \sum_{j\in B} \mathbf{S}_j)^2 \right\rangle \qquad (2)$$

where the two summations are taken over lattice sites belonging to different sublattices, as shown in Fig. 1. The dependence of the values of the above observable on J_2, allows one to identify any range of parameters in which possibly magnetically disordered phases may exist. It is worth restating that in this work we consider only two types of magnetic long-range order, schematically illustrated in Fig. 1, namely Néel and collinear.

Figure 3 shows estimates of the Néel SSM extrapolated to the thermodynamic limit (left part), based on the functional form $\mathbf{m}^2(N, l, J_2) = \mathbf{m}^2(\infty, l, J_2) + \beta(l, J_2)N^{-1/2}$,

for different plaquette sizes. Just like for the energy, the right part of the figure shows the extrapolated values $\mathbf{m}^2(\infty, l, J_2)$, this time plotted versus $l^{-1/2}$. The fit to the data is performed using a quadratic functional dependence (dashed lines).

For $J_2 = 0$, our estimates in the large l limit is again in quantitative agreement with QMC ones[13,18]. At $J_2 = 0.15$ the Néel SSM is finite; we make such a statement based on the observation that assuming a linear dependence of $\mathbf{m}^2(\infty, l, J_2)$ on $l^{-1/2}$ (the fit is acceptable), we obtain a finite extrapolated value [dotted line in Fig. 3 (right part)]. On including a term proportional to l^{-1} the visible upward bend of the data is better described. In turn, the extrapolated value of the order parameter increases.

For $J_2 = 0.2$ a linear fit gives an unphysical value while a quadratic one gives a better description of the data leading, within the accuracy of our calculation, to a null value of the Néel order parameter. Therefore it is reasonable to locate the transition point, at which the Néel order vanishes, very close to $J_2 = 0.2$.

For $0.2 \lesssim J_2 \lesssim 0.4$ we find no evidence of magnetic order (either of the Néel or collinear type), whereas for
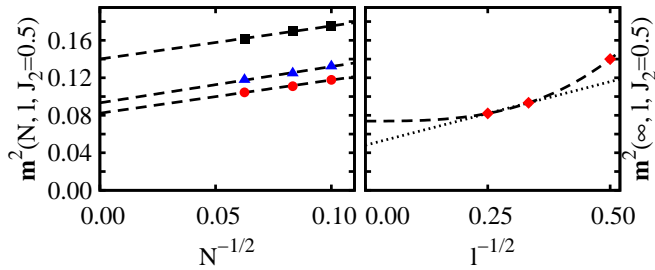
FIG. 4: (color on line). Same of Fig. 3 for $J_2 = 0.5$. Here A and B sublattices are chosen as in the right part of Fig. 1. The dependence of the collinear order parameter on the plaquette size is described by using a function which includes besides the zero-th order, orders higher than the quadratic (in $l^{-1/2}$) one (dashed line) and only the linear one, excluding the point at $l = 4$ (dotted line). Both descriptions yield, when l is saturated, a finite collinear SSM.
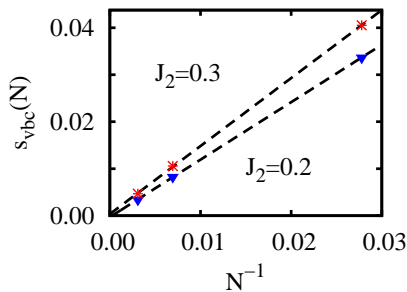

FIG. 5: (color on line). Finite size scaling of the plaquette valence-bond crystal order parameter for two values of J_2 at which the system is found in a magnetically disordered GS. Dashed lines are fits to the numerical data with the same J_2. This order parameter clearly vanishes, for all the l values considered in this work, in the thermodynamic limit. Data shown refer to the $l = 16$ case.

larger J_2, the GS of the system orders collinearly.

Figure 4 shows the collinear SSM as a function of N (left part), and its values extrapolated to the thermodynamic limit versus l (right part), for $J_2 = 0.5$. The right panel shows that the collinear order parameter is finite. Collinear order has been found up to $J_2 = 1.0$ (i.e., the maximum J_2 value considered in this study).[19]

Our prediction of Néel order persisting up to $J_2 \sim 0.2$ is in agreement with recent ED works.[5,6] That the collinearly ordered phase appears at $J_2 \sim 0.4$ is also consistent with the ED suggestion.[6] As shown by our energy estimates (Tab. I), the collinear phase is favored with respect to the dimerized rotational-symmetry breaking one (described via a resonating valence-bond WF) proposed for $J_2 \gtrsim 0.3$ in Ref. 4. ED studies also predict a plaquette valence-bond crystal phase in the region in which neither Néel nor collinear orders occur. By estimating the appropriate order parameter, defined as in Ref. 5, we find this kind of order in the region of interest, only in systems of small size, i.e., the plaquette structure factor is found to vanish in the thermodynamic limit (see Fig. 5). Therefore, our best GS candidate in this parameter window, is disordered (spin liquid). A disordered GS has been also found by the authors of Ref. 4. Such a phase, however appears at a value of the NNN coupling constant approximately two times smaller than that found by us.

Summarizing, the $J_1 - J_2$ model on the honeycomb lattice has been investigated by means of variational calculations based on the EPS WF. The phase diagram of the model displays three distinct regions: magnetic order of Néel and collinear type is found for $J_2 \lesssim 0.2$ and $J_2 \gtrsim 0.4$ respectively; in the intermediate region, none of the ordered parameters considered here remains finite, consistently with a disordered GS scenario. Such a disordered region has been not revealed by ED studies, in our view, due to the small size of the lattices that are accessible to them. Interestingly, the value of J_2 at which Néel order vanishes, according to both ED and our calculations, is considerably larger than that ($J_2 \simeq 0.08$) found in Ref. 4. In Ref. 4, a striking similarity was suggested between the phase boundary of the $J_1 - J_2$ and that of the half-filled Hubbard model[14] at the Neel-to-disorder transition; the validity of such a suggestion may have to be reconsidered, in the light of the results presented here which indicate that the simple reduction of the physics of the Hubbard model to that of an effective spin-1/2 system, such as the $J_1 - J_2$, might not be achievable.

[1] J. Struck, C. Ölschläger, R. Le Targat, P. Soltan-Panahi, A. Eckardt, M. Lewenstein, P. Windpassinger and K. Sengstock, Science **333**, 996 (2011).

[2] Henceforth, we set the value of the NN AF coupling constant J_1 to unity, and take it as our energy unit.

[3] V. Murg, F. Verstraete and J. I. Cirac, Phys. Rev. B **79**, 195119 (2009) and references therein.

[4] B. K. Clark, D. A. Abanin and S. L. Sondhi, Phys. Rev. Lett. **107**, 087204 (2011).

[5] H. Mosadeq, F. Shabazi and S. A. Jafary, J. Phys. Condens. Matter **23**, 226006 (2011).

[6] A. F. Albuquerque D. Schwandt, B. Hetényi, S. Capponi, M. Mambrini and A. M. Läuchli, Phys. Rev. B **84**, 024406 (2011).

[7] A. Mulder, R. Ganesh, L. Capriotti and A. Paramekanti, Phys. Rev. B **81**, 214419 (2010).

[8] J. Reuther, D. A. Abanin and R. Thomale, Phys. Rev. B **84**, 014417 (2011).

[9] D. C. Cabra, C. A. Lamas and H. D. Rosales, Phys. Rev. B **83**, 094506 (2011).

[10] J. Oitmaa and R. R. P. Singh, Phys. Rev. B **84**, 094424 (2011).

[11] Y.-M. Lu and Y. Ran, Phys. Rev. B **84**, 024420 (2011).

[12] H. Y. Yang and K. P. Schmidt, Eur. Phys. Lett. **94**, 17004 (2011).

[13] A. W. Sandvik, Phys. Rev. B **56**, 11678 (1997); E. V. Castro, N. M. R. Peres, K. S. D. Beach, and A. W. Sandvik Phys. Rev. B **73**, 054422 (2006).

[14] Z. Y. Meng, T. C. Lang, S. Wessel, F. F. Assaad and A. Muramatsu, Nature **464**, 847 (2010).

[15] F. Mezzacapo, N. Schuch, M. Boninsegni and J. I. Cirac New J. Phys. **11**, 083026 (2009).

[16] F. Mezzacapo and J. I. Cirac, New J. Phys. **12**, 103039 (2010); F. Mezzacapo, Phys. Rev. B **83**, 115111 (2011); H. J. Changlani, J. M. Kinder, C. J. Umrigar and G. Kin-Lic Chan, Phys. Rev. B **80**, 245116 (2009); S. Al-Assam, S. R. Clark, C. J. Foot and D. Jaksch, Phys. Rev. B **84**, 205108 (2011).

[17] The large l limit of our estimates is achieved by using, starting from plaquettes of a given size (in our case four sites), data obtained with plaquettes whose size is systematically and consistently increased (i.e., by considering plaquettes with $2l^{1/2} + 1$ more sites each time that the plaquette size l is changed).

[18] J. D. Reger, J. A. Riera and A. P. Young, J. Phys. Condens. Matter **1**, 1855 (1989).

[19] For $J_2 \to \infty$ the Hamiltonian studied here reduces to that of two decoupled antiferromagnets on the triangular lattice which features $2\pi/3$ long-range ordered GS, therefore, such a GS has to emerge when the NNN interaction becomes dominant.[20]

[20] C. N. Varney, K. Sun, V. Galitski and M. Rigol, Phys. Rev. Lett. **107**, 077201 (2011).